SUPERSONIC WING / BODY INTERFERENCE

S.C.Blank
College of Aeronautics,
Cranfield, Bedford, U.K.

ABSTRACT

An experimental investigation of glancing shock wave / turbulent boundary layer interaction produced by hemi-cylindrically blunted swept (45°) and unswept fins was conducted at a Mach number of 2.45 and a Reynolds number (Re_δ) of 4.1×10^4. In an attempt to weaken the interaction strength fillets were used which created significant alterations to the flow field structure. The study involved mean static pressures measured on the side wall, surface oil flow pictures taken over the side wall and the fin, and schlieren pictures taken in two planes normal to each other.

INTRODUCTION

The interaction between the bow shock wave generated by a blunt leading edge wing and the turbulent boundary layer growing over the fuselage can create many problems for the aircraft designer. Firstly, due to the adverse pressure gradients created in the subsonic section of the boundary layer separation occurs and a number of vortices are formed. The number of which depends upon the value of the freestream unit Reynolds number [2,3]. Secondly, the bow shock bifurcates forming shock / shock interaction [1]. Thirdly, the peak static pressures created around the leading edge can be as large as six times the freestream value. Furthermore, local flow field unsteadiness within the interaction region creates an additional complication.

The current research is aimed at illustrating the effects of junction modifications on the flow field by the introduction of fillets for straight and swept wings. Lakshmanan [4] in a computational study has produced the only known contribution at supersonic speeds to this important field. In his paper fillets of circular profile were used but only extremely large fillets of radius 3.5D (D being the fin leading edge diameter) were found to have a significant weakening effect. Unfortunately, no experimental data existed from which he could evaluate his code for the filleted interactions. This paper is aimed at bridging this gap in knowledge for these important flows.

EXPERIMENTAL DETAIL

The experiments were conducted in the College of Aeronautics' continuous supersonic wind tunnel at a Mach number of 2.45 and at zero incidence. The tunnel stagnation pressure and temperature were 0.25 bar and typically 300° K respectively. The test section Reynolds number, Re_δ, was 4.1×10^4 and the fully developed turbulent boundary layer growing under a zero pressure gradient along the working section walls [5] and a 99.5% thickness (δ) of 1.6cm. The corresponding displacement and momentum thicknesses were 0.38 and 0.10 cm.

The experimental arrangement is displayed in fig.1 and the models are sketched in fig.2. Fillets were manufactured so that the plain fins ($D/\delta = 1.6$) could be placed on the fillet's upper surface, increasing the aspect ratio of the combination fin relative to that of the plain fin. The fillet details are illustrated in fig. 2b. The fin models had semi-circular leading edges in the plane normal to the leading edge (i.e. elliptic in the freestream direction for the swept model) [6,7].

Surface oil flow patterns were formed using a mixture of titanium dioxide and motor oil with a few drops of oleic acid added to avoid coagulation. In order to give good photographic contrast the models were painted matt black. The oil patterns on the side wall were photographed whilst the tunnel was running but the fin side view patterns had to be captured after tunnel shut down because of the tunnel's physical constraints and this,occasionally, resulted in some slight smearing.

Single pass schlieren tests were conducted with the model mounted vertically in contact with the upper working section liner, and horizontally, with the fin base almost touching the glass window. During the horizontal tests a gap of 0.2 mm was left between the glass window and the model base at atmospheric conditions to allow for any window deflections resulting from the differential pressure loading occurring during tunnel running. A microsecond spark source was used to generate the light beam and the shock patterns were recorded on HP5 400 ASA film loaded in an Olympus camera.

Detailed surveys of the mean surface static pressure distribution in the interaction region were made by means of an

array of pressure ports drilled in a turn-table (fig. 1). Each of the 226 ports were connected in turn via a scanivale to a Druck PDCR 22 (15 psia) pressure transducer. The ports were scanned slowly with up to one second being allocated for settling time and the model's position was shifted between different tests to increase the effective density of the ports. The pressure transducer signals were amplified, digitized and displayed by an on-line computer which also stored the data onto floppy discs. Ten readings were then taken for each port and the average value was downloaded from a MINC minicomputer via a VAX 750 to a UNIX work-station.

RESULTS AND DISCUSSION

Case 1 : The Blunt Unswept Fin

Numerous previous investigators [1,2,3,6,7] have described in some considerable detail the development of glancing interaction. Leading edge bluntness causes the bow shock wave to detach and the two sides of the fin can communicate more easily than in the sharp fin case. A normal shock wave will be generated and local separation at the root is likely. Local separation will, in turn feed forward through the subsonic section of the boundary layer and modify the shape of the bow shock creating a lambda foot.

Some indication of the complexity of the flow field can be gained from the oil flow photograph, fig.3. Viewed from above the fin, fig.3 suggests that the four vortex model proposed by Sedney and Kitchens [3] is applicable to the present case and the pattern on the side of the fin is similar to those recorded in refs. 6 & 8.

The horizontal schlieren photograph fig.4, indicates the existence of a double bow shock system as opposed to a single shock wave. The upstream shock's position was found to correspond to the stand-off distance of the bow shock wave in the vicinity of the triple point. Likewise, the rear image was found to relate to the downstream leg of the lambda foot.

Details of the flow in the root region are shown in fig.5. These schlieren photos clearly indicate the gross local unsteadiness of the separation shock structure and the movement of the triple point. Note that there are a considerable number of compression waves present around the numerous shocks. The triple point undergoes a vertical plane motion of about 0.6D (δ). Blank [9] working in a different wind tunnel at M = 2.3, δ = 6 mm and $Re_\delta = 5.8 \times 10^4$ on a hemi-cylindrically blunted strut of $D/\delta = 0.\bar{7}$ found that the jet's origin (i.e. the triple point) underwent a height change of 0.3D (0.2δ). Clearly, D/δ is a parameter of great importance to this motion.

Further observations of the lambda foot reveal that the separation shock's amplitude is about D and the rear leg undergoes a similar curling motion to that mentioned in ref.9. Both Dolling [10] (at M = 2.95) and Blank [9], have found that the separation shocks traverse a distance of approximately D and therefore, the separation shock's amplitude appears to be independent of δ, Re and small Mach number changes.

Case 2 : The Blunt Filleted Unswept Fin

The side wall oil flow pattern, fig.6, indicates that the fillet induces an upstream movement to the primary separation line, S_1, and the upstream influence line, U, relative to the fin alone case. This movement is clearly indicated by comparing the position of the primary separation lines in figs. 3 and 6 to the turn-table joint T. A third separation line, S_3, is also easily distinguished around the fillet / wall interface and it's accompanying attachment line, A_3, is quite readily recognised close to the fin leading edge. The separation line S_3 leaves the fillet / side wall interface once the region of curvature has been passed and it gradually climbs the fillet in an elongated "S" like manner. Concurrently, the attachment line A_2 leaves it's position near to the fillet / wall interface and approaches S_2, the secondary separation line. Between A_2 and S_3 one would normally expect to find a small vortex rotating in the opposite sense to the primary vortex. This expectation is supported by the close proximity of the two lines whilst in the region of curvature, but once past this region, a sudden, unexplained, increase in the distance between these two lines occurs.

The nodal point of attachment (NPA) for the non-filleted fin reported in Stollery et al [8] is still present, in the same position, on the fin leading edge. Also, the jet which Fomison [6] and Stollery et al [8] mention, and Winkleman [11] acknowledges, appears to be relatively unaffected by the introduction of the fillet, fig.7.

A comparison of the side view schlieren pictures tends to indicate that the fillet has weakened the separation shock / compression wave structure (fig.8). The distance over which the triple point traverses is 1.3δ but this figure is based upon the highest compression wave / bow shock wave intersection point. If one however, considers the amplitude of distinctive shock waves (fig.8a) as opposed to weak compression waves (fig.8b) then the amplitude of the triple point is reduced to 0.9δ. Regardless of the measuring criteria, the amplitude of the triple point is still similar to that in

the non-filleted example and, it is worthwhile to note, that the mean position of the separation shock wave is closer to the base of the fin than in the non-filleted case above.

The fillet does not affect the separation shock's amplitude which remains as about D. The up- and downstream bounds of the motion being the primary and secondary separation lines. Interestingly, this region in the oil flow pictures suffers from poor resolution in comparison to the other areas, and this maybe linked to the unsteady shock motion.

The fillet has a number of effects upon the bow shock wave which the superimposing of the shocks in fig.9 shows. The bow shock is pushed slightly upstream, within the areas that can be viewed, and in the far field region, a significant broadening of the shock system has been introduced. These points are indicative of a possible weakening of the shock system but further experimental data is required before a categoric statement can be made.

Case 3 : The Blunt Swept Fin

Price and Stallings[11] reported the effects of sweep on glancing interaction as long ago as 1967. Upon the introduction of sweep the centre-line pressure distribution collapses (fig.10) and the disturbed area (defined by the primary separation line) contracts (fig.11)[2].

Hussain[7] examined blunted fins at various sweep angles up to 75° and incidence angles from 0 to 24° at the same test conditions as the present study. He confirmed the benefits of sweep in greatly reducing the level and extent of the disturbed pressure field (fig.12). The characteristic double peaked pressure signature is reduced dramatically in scale as the sweep is increased[2] and the effects of sweep on the whole flow field for the non-filleted models is quite significant as illustrated in fig.13. Hussain's and the present oil flow pictures (fig.14) indicate that separation is still occurring at 45° of sweep. Moreover the flows are unsteady and it is to this we shall now turn.

The triple point appears to undergo a height variation of about δ whilst the separation shock is located roughly 0.5D upstream of the fin root (fig.15). The shock structure is still locally unsteady but the areas involved have been reduced. The separation and rear lambda shocks appear to be considerably weaker than their unswept counterparts in fig.5. In brief, not only does sweep reduce the mean properties of the interaction it also reduces the unsteadiness of the shock / shock interaction, limiting it to within about a diameter vertically and approximately half a diameter ahead of the fin root.

The schlieren image of the bow shock wave (fig.16) indicates that the bow shock is diffuse in the neighbourhood of the leading edge. Hussain[7] conducted a series of experiments with delta wings but none of his results, which are not presented here, indicate any similar effects within this region. Extrapolating the bow shock in fig.15, reveals that a locally attached shock will be formed at the root as in Hussain's delta wing experiments. It is therefore believed that the bow shock becomes fainter in the leading edge region as a direct result of the shock wave / boundary layer interaction (fig.16). When extrapolated the path of the bow shock in fig.15 is only a small distance ahead of the rear lambda shock's foot. This small distance will increase as the distance from the centreline is increased due to the quasi-conical state of the flow. Hence the gradual thickening, and possible weakening, of the shock structures as the tunnel walls are approached.

Case 4 : The Blunt Filleted Swept Fin

The oil flow patterns for the filleted swept fin (fig.17) are much more complex than those without the fillet[7]. The primary separation line is extremely well-defined but it's accompanying attachment line has poor resolution. Secondary separation is indicated by a region of high skin friction and it's reasonably well-defined attachment line appears in the vicinity of the fillet / wall interface.

The patterns on the fillet and fin are very complex (fig.18) and the interpretation of the lines in certain regions, notably the front of the fillet, will not be considered at this stage. Certain distinctive features are easily identified, and one of these is the nodal point of attachment (NPA). Sweep causes the NPA to approach the fin root and the introduction of the fillet produces a single NPA located close to the root of the fillet (fig.17).

A distinctive separation line, S_4, and an accompanying attachment line, A_4, appear in front of the fin's leading edge. The separation line, S_4, gradually descends the fillet as it passes around the fin leading edge. Another separation line, S_3, leaves the fillet / wall interface where it is located whilst in the curvature zone, and climbs up the fillet (at a much faster rate than in unswept filleted example above) once past the end of the fillet curvature. Eventually, S_3 and S_4 intersect but only a single separation line can be seen emerging from the intersection point. This intersection cannot, at present, be explained.

The path of the "jet like region" is altered considerably. It no longer climbs up the fin along the edge of the fin's curvature, as in fig.14, but it passes, instead, initially along the fin / fillet interface, for about 0.5D, before ascending the fin. This results in a reduction in the disturbed fin flow of about 15%. Before the flow features of this combination fin can be adequately described in sufficient detail to warrant usage of fillets on aircraft, further detailed experiments, including three-dimensional flow field visualisation studies and mean static pressure surveys, are required.

The vertical schlieren images indicate that a substantial change in the shock structure occurs upon the introduction of the fillet. A "lambda foot" still exists. The rear leg of which is reasonably steady whilst the lower part of the front leg suffers from local unsteadiness due to turbulent fluctuations in the separated shear layer and / or boundary layer flow, fig.19. The unsteady regions are in total much smaller than those without fillet and only occasionally can weak compression waves be viewed ahead of the fillet's leading edge. The unsteady flow regime being mainly concentrated on the fillet and at the fin / fillet interface. A weak image of what can be interpreted as the jet is also present on the photographs and its thickness expands as it gets further from the triple point.

The superimposed bow shock profiles in fig. 20 show that the filleted interaction covers a larger area and that the fillet pushes the bow shock wave, within the areas that can be viewed, upstream.

CONCLUSIONS

Experiments have been conducted to investigate the effect of introducing fillets into swept and unswept fin / fuselage junctions at supersonic speeds. Significant flow field changes have resulted. The flow on the fillet is very complex.

Sweep was found to decrease not only the mean properties of the flow field, but also the scale of the unsteadiness. The amplitude of the straight fin's separation shock was found to be about D. The introduction of the fillet did not alter the magnitude of the separation shock's amplitude nor did it significantly affect the triple point's amplitude which remained as approximately δ. The shape of the lambda foot produced by the swept fin was considerably changed upon the introduction of the fillet. In both cases the fillet generated a broader shock system and the region of separated flow increased.

To more fully understand these complex flow fields three-dimensional visualisation studies and further mean static pressure surveys are required.

ACKNOWLEDGEMENTS

This paper is dedicated to the memory of the author's Grandfather, Mr.Alwyn Garside, who passed away unexpectedly earlier this year, on the 23rd February, whilst the author was in the midst of conducting the experiments whose results are presented herein.

The author is indebted to his supervisor, Prof.J.L.Stollery and the College's technical staff for their constant help and advice. The generosity of the Royal Aeronautical Society, British Airways, The Fellowship of Engineering and SERC have made the presentation of this paper possible and the author wishes to thank them for their outstanding kindness.

REFERENCES

1. Edney,B., 1968, "Anomalous Heat-Transfer and Pressure Distributions on Blunt Bodies at Hypersonic Speeds in the Presence of an Impinging Shock". FFA Report no.115.

2. Stollery,J.L., 1989, "Glancing Shock-Boundary Layer Interactions", AGARD Report No.764 - Special Course on Three-Dimensional Supersonic / Hypersonic Flows Including Separation. FDP/VKI/CPP.

3. Sedney,R., and Kitchens,C.W., 1977 "Separation Ahead of Blunt Protuberances in Supersonic Turbulent Boundary Layers", AIAA J., Vol.15, No.4, pp.546-552,April 1977.

4. Lakshmanan,B.,Tiwari,S.N. and Hussaini, M.Y., 1988, "Control of Supersonic Interaction Flowfields Through Filleting and Sweep". AIAA/ASME/SIAM/APS First National Fluid Dynamics Congress,July 1988.

5. Kubota,H., 1980, "Investigation of Three Dimensional Shock Wave Boundary Layer Interactions", PhD Thesis College of Aeronautics, Cranfield Institute of Technology. See also Kubota,H. and Stollery, J.L., 1982,"An Experimental Study of the Interaction Between a Glancing Shock Wave and a Turbulent Boundary Layer". Journal of Field Mechanics, Vol.116,p.431-458.

6. Fomison ,N.R.,1986, "The Effects of Bluntness and Sweep on Glancing Shock Wave Turbulent Boundary Layer Interaction" PhD Thesis College of Aeronautics, Cranfield Institute of Technology, See also Fomison,N.R. and Stollery, J.L. 1987, "The Effects of Sweep and Bluntness on a Glancing Shock Wave Turbulent Boundary Interaction", AGARD CP 423.

7. Hussain,S.,1985, "A Study of the Interaction Between a Glancing Shock Wave and a Turbulent Boundary Layer - The Effects of Leading Edge Bluntness and Sweep", PhD Thesis College of Aeronautics, Cranfield Institute of Technology, November 1985.

8. Stollery,J.L. Fomison,N.R. and Hussain,S., 1986, "The Effects of Sweep and Bluntness on Glancing Interactions at Supersonic Speeds", ICAS-86-1.2.1.

9. Blank,S.C., 1991, "Glancing Interaction", MSc Thesis College of Aeronautics, Cranfield Institute of Technology, September 1991.

10. Dolling,D.S. and Bogdonoff,S.M.,1981, "An Experimental Investigation of the Unsteady Behaviour of Blunt Fin-Induced Shock Wave/Turbulent Boundary Layer Interactions", AIAA Paper 81-1287.

11. Winklemann,A.E., 1972, "Experimental Investigations of a Fin Protuberance Partially Immersed in a Turbulent Boundary at Mach 5", NOLTR-72-33.

12. Price,A.E. and Stallings,R.L. 1967, "Investigation of Turbulent Separated Flows in the Vicinity of Fin Type Protuberances at Supersonic Mach Numbers", NASA TN-D-3804.

FIGURES

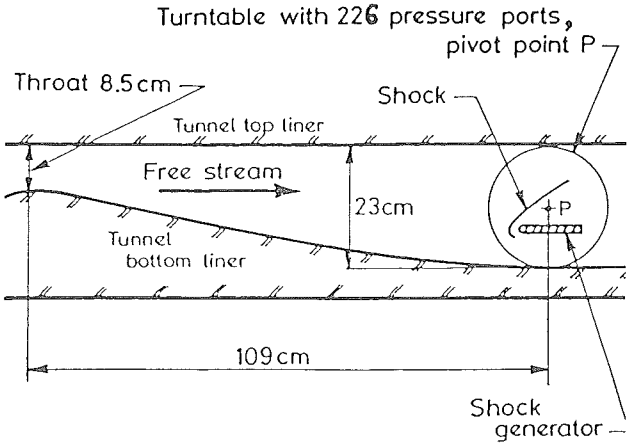

Fig.1 Experimental arrangement in the 23 cm x 23 cm wind tunnel.

The Plain Straight Fin

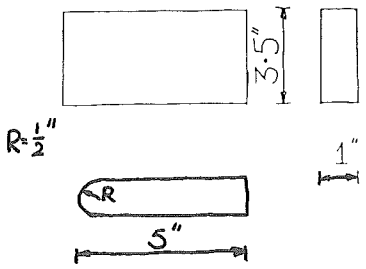

The Plain Swept (45°) Fin

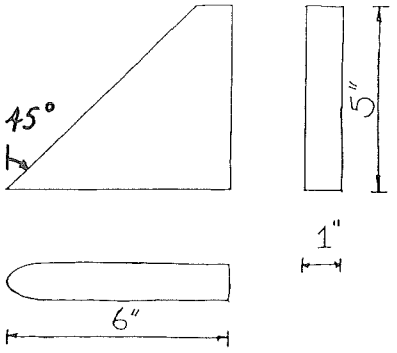

Fig. 2a Model details

The Straight Fin's Fillet

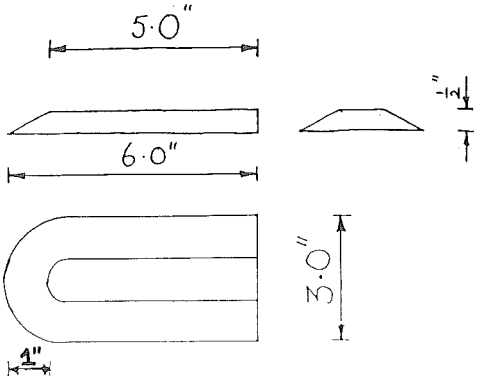

The Swept Fin's Fillet

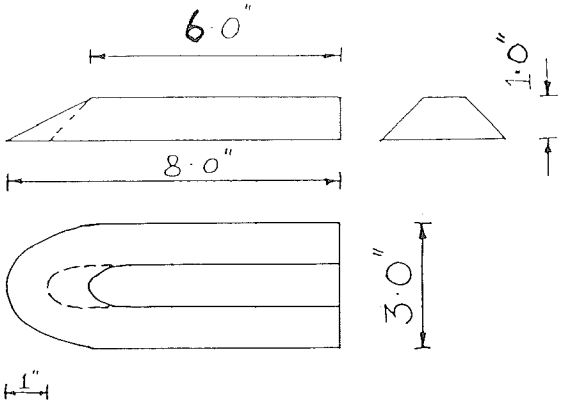

Fig. 2b Fillet details

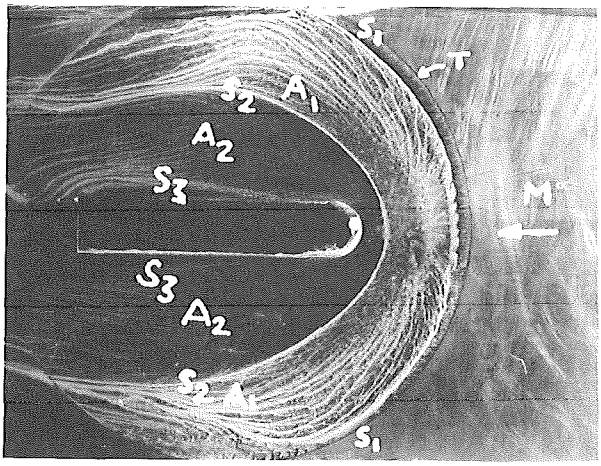

Fig.3 Side wall oil flow photograph for the straight fin without fillet

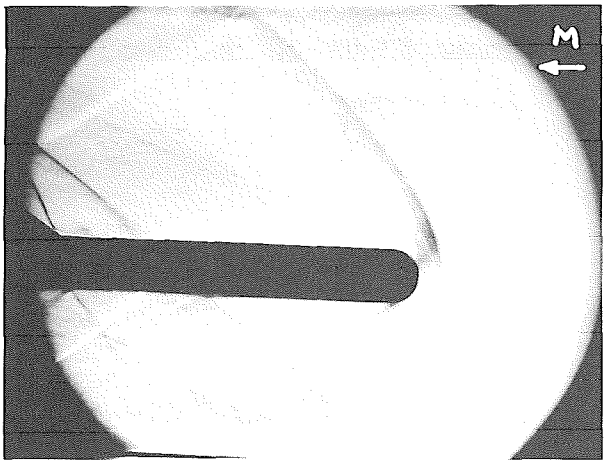

Fig.4 Horizontal schlieren image for the unswept fin without fillet

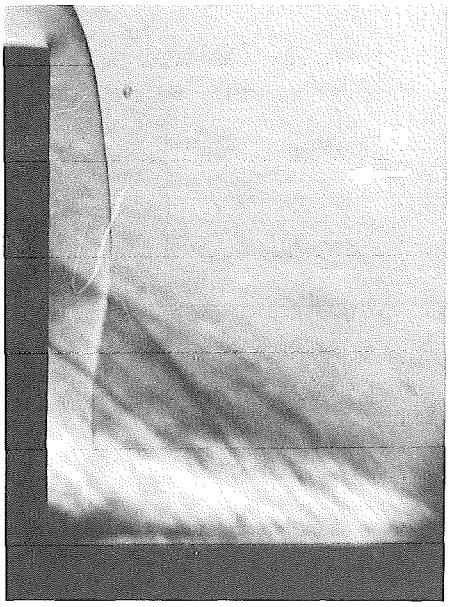

(a)

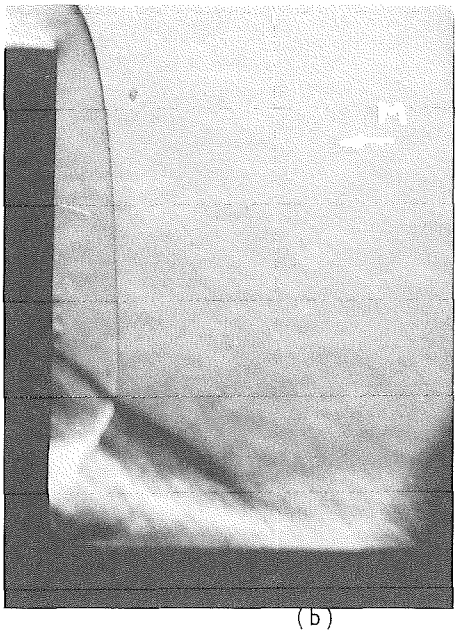

(b)

Fig. 5 Vertical schlieren photos of the unswept fin without fillet

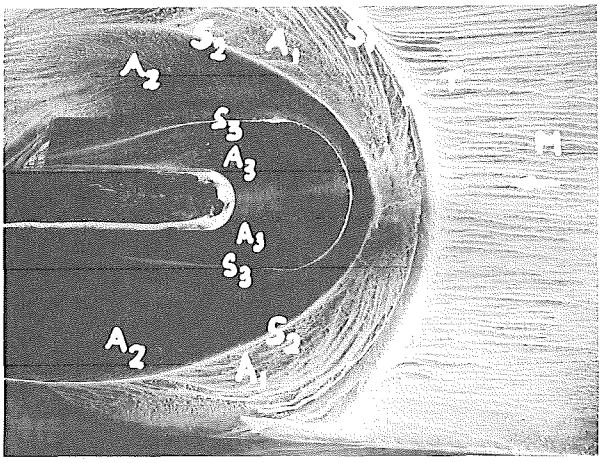

Fig.6 Side wall oil flow picture for the straight fillet fin.

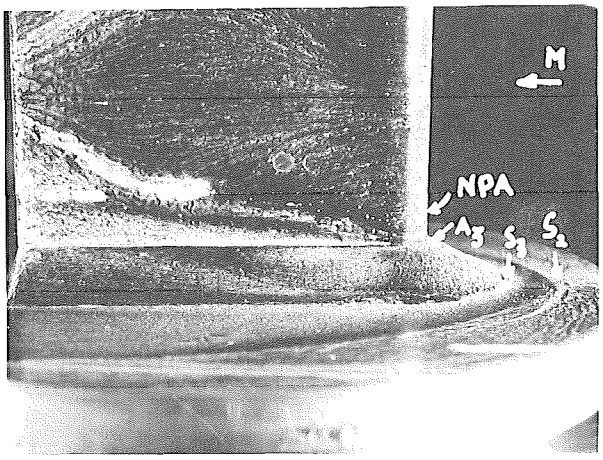

Fig.7 Fin side view oil pattern

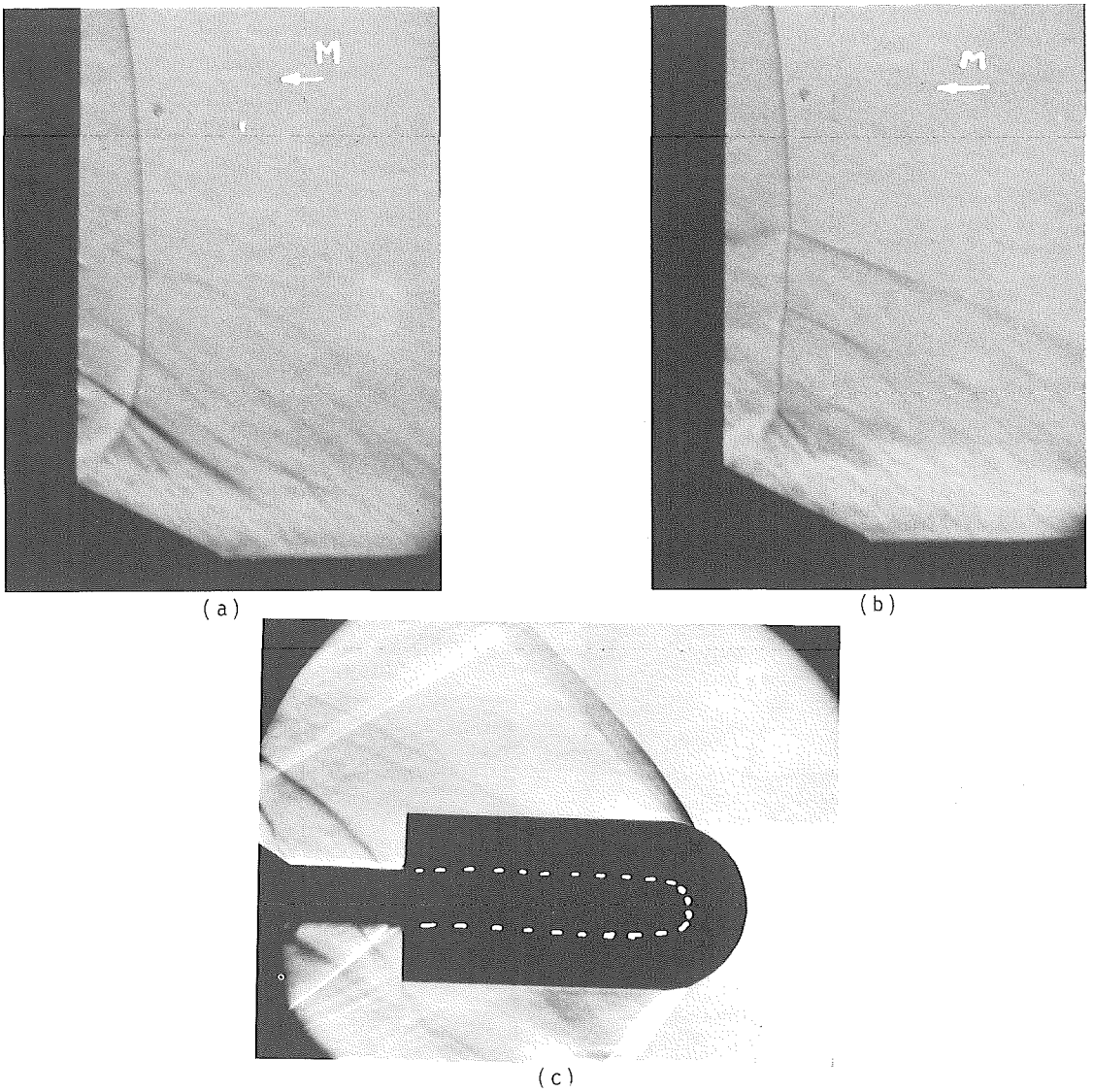

Fig. 8 Vertical (a & b) and horizontal (c) schlieren images of the filleted unswept fin

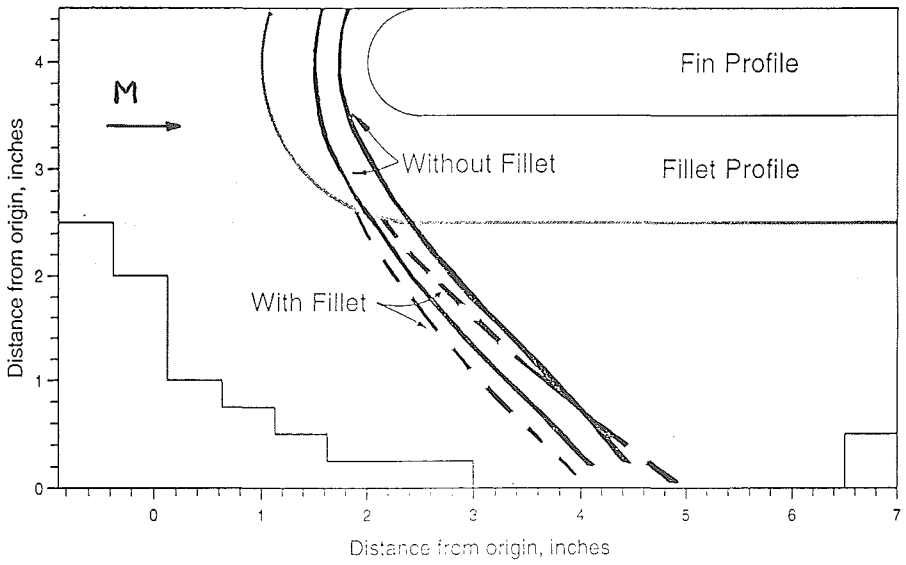

Fig. 9 Superimposing of the bow shocks for the unswept models

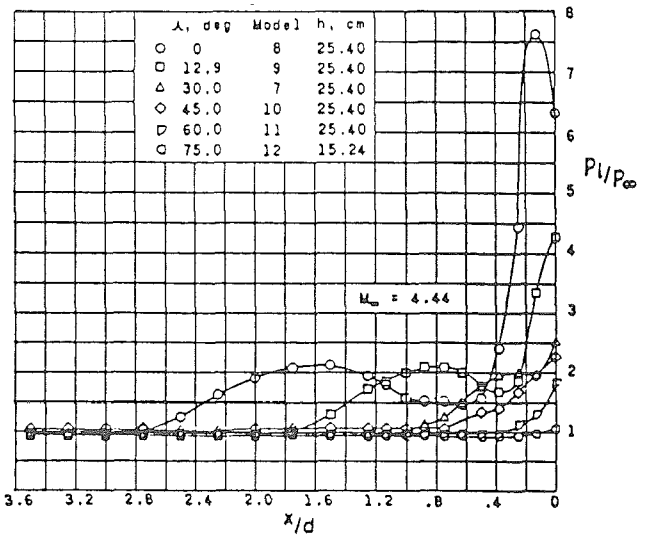

Fig.10 The effect of sweep on the pressure distribution along the line of symmetry of a blunt fin (from ref.2)

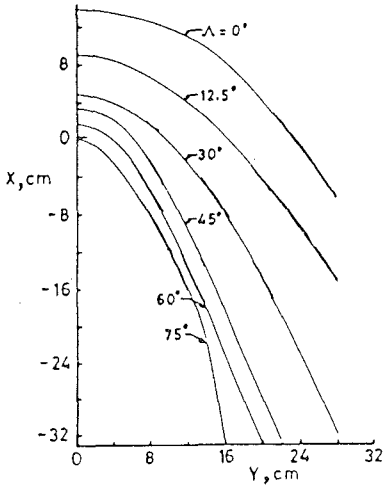

Fig.11 The effect of sweep on the primary separation lines around a blunt fin, D=2" = 5.08cm (from ref.12)

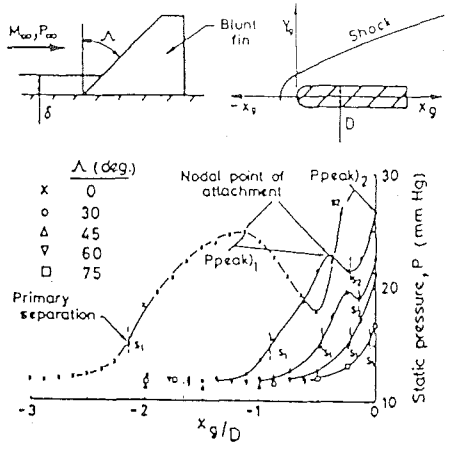

(a) Centre Line Pressure Distribution, D = 1in, α = 0°, Yg/D = 0

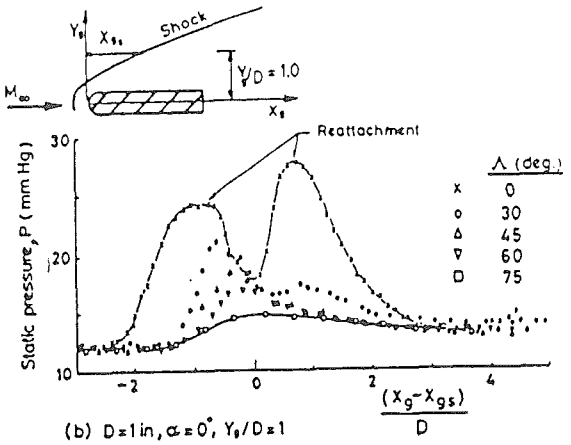

(b) D=1in, α=0°, Yg/D=1

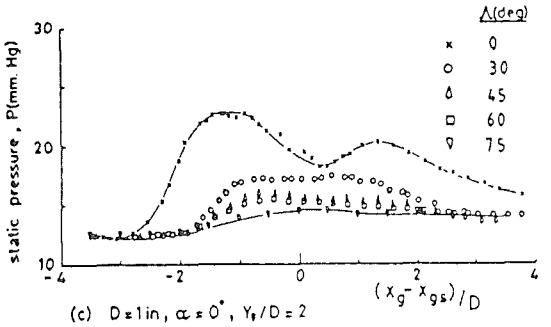

(c) D=1in, α=0°, Yg/D=2

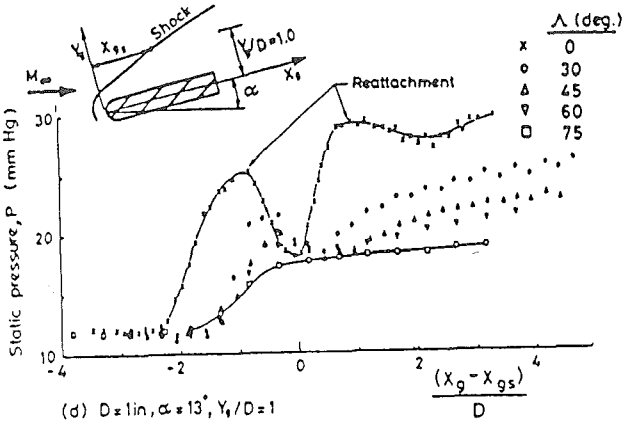

(d) D=1in, α=13°, Yg/D=1

Fig.12 The effects of sweep on the wall pressure distributions generated by a blunt fin (from ref.7)

(a) Pressure contours for the straight fin

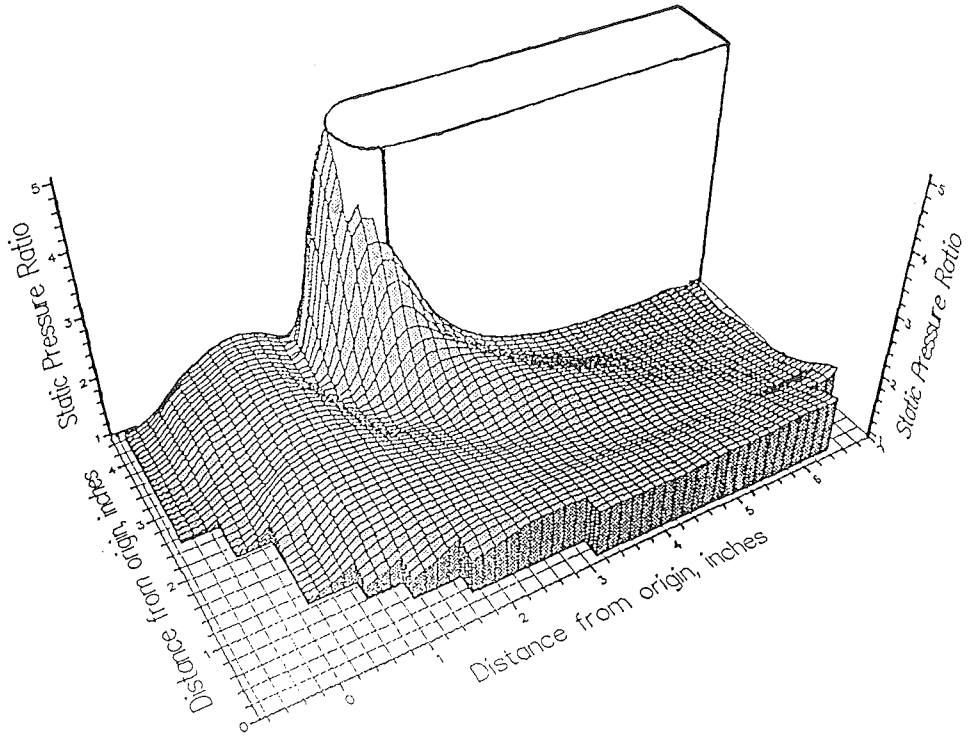

(b) Pressure contours for the 45° swept fin

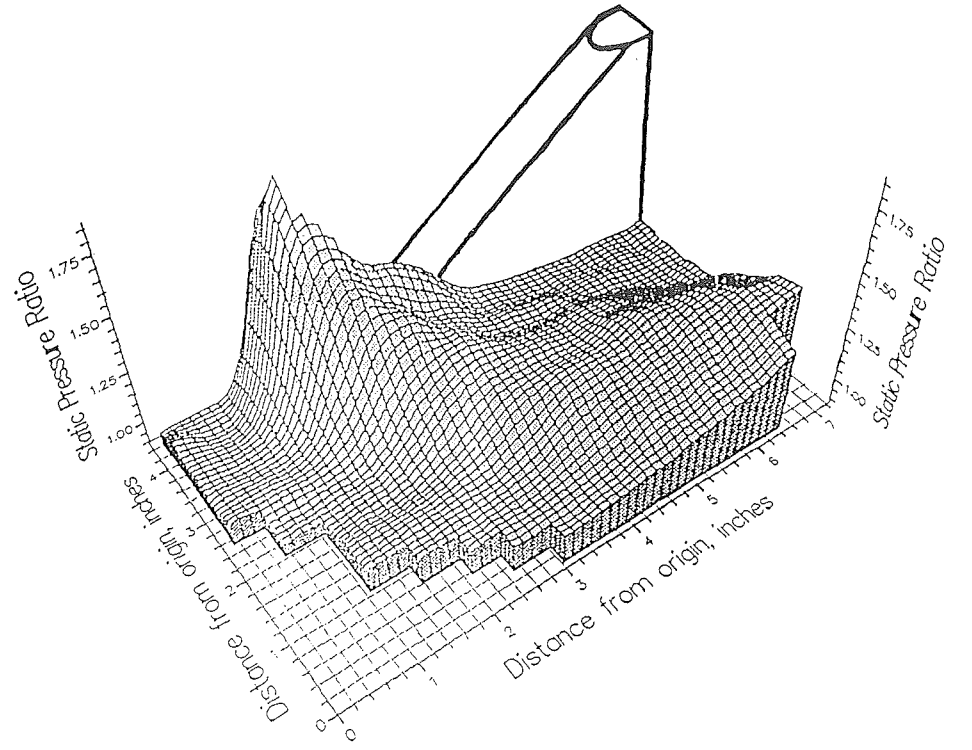

Fig. 13 Pressure countour plots for the plain models

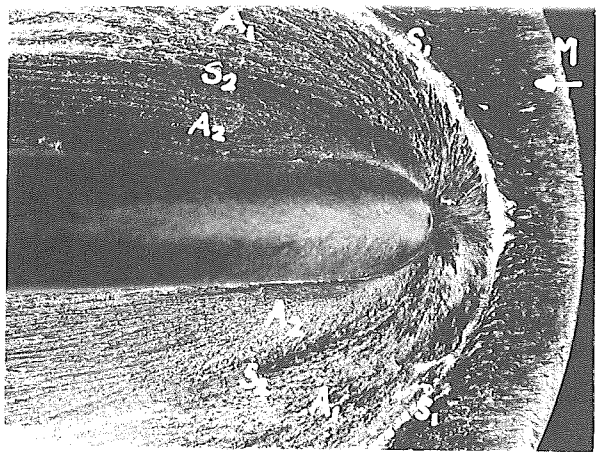

Fig. 14 Side wall oil flow pattern for the swept fin without fillet

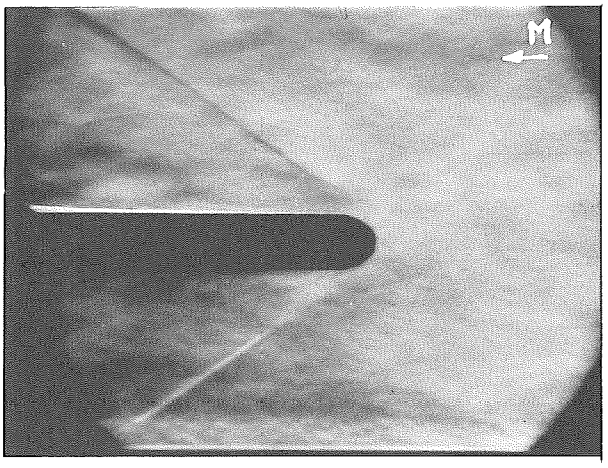

Fig. 16. Horizontal schlieren image for the swept fin without fillet

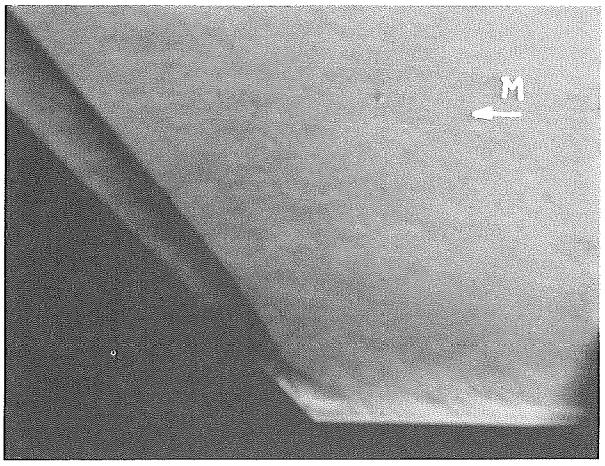

(a)

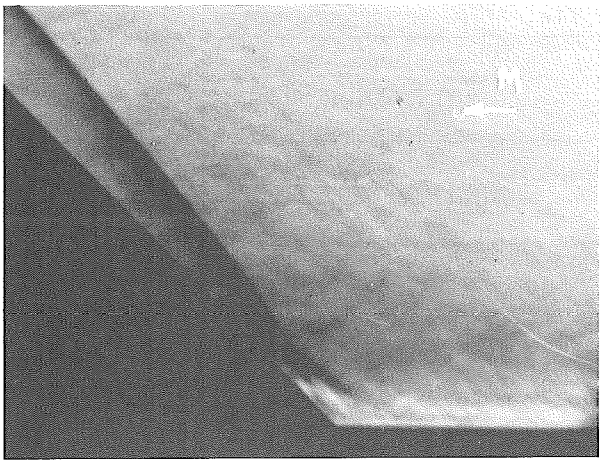

(b)

Fig. 15 Vertical schlieren images of the swept fin without fillet

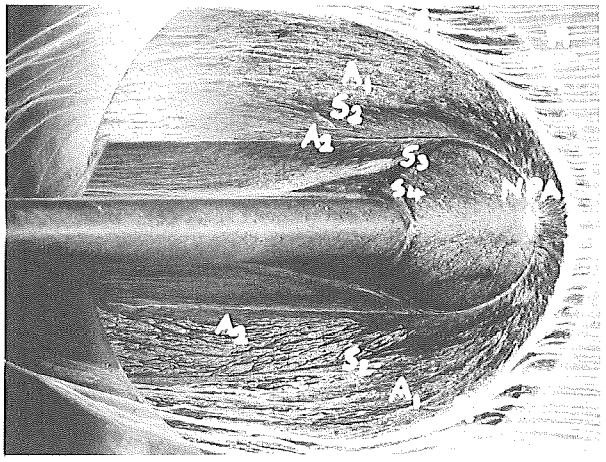

(a)

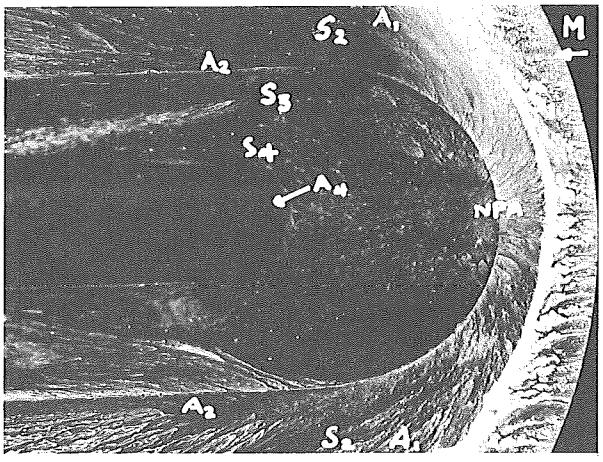

(b) close-up of the fillet's leading edge

Fig. 17 Wall oil flow pictures for the swept fin with fillet

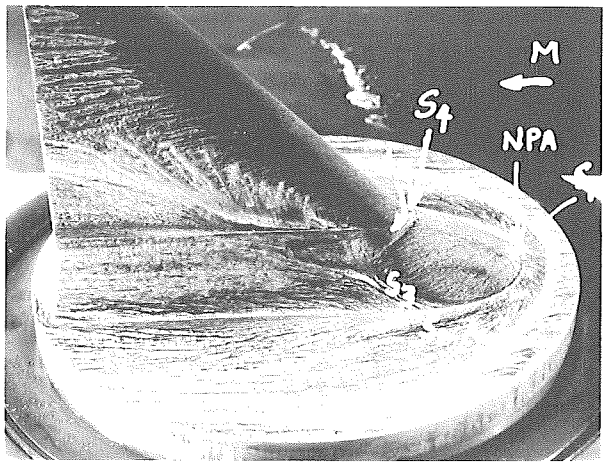

Fig. 18 Side view of the oil flow pattern generated by the swept filleted fin.

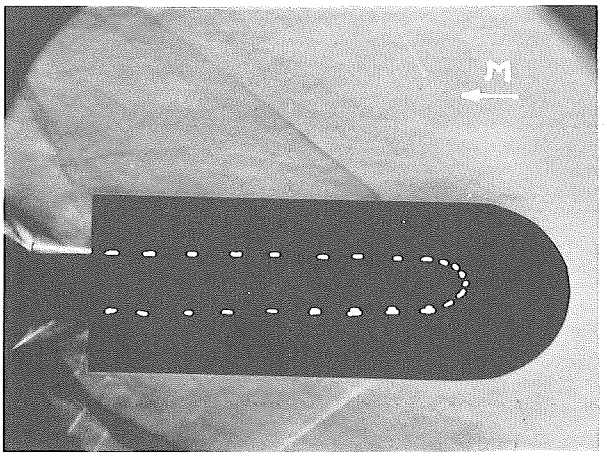

(a)

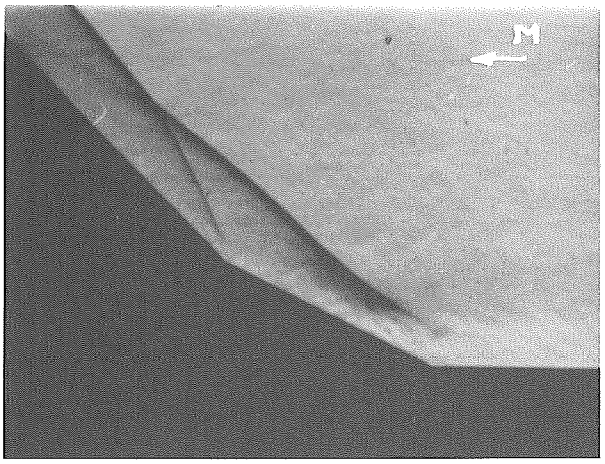

(b)

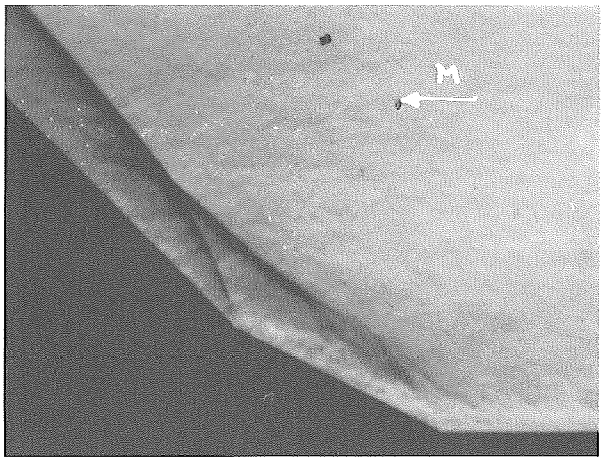

(c)

Fig. 19 A horizontal schlieren image (a) and high magnification vertical schlieren images (b & c) of the swept filleted fin.

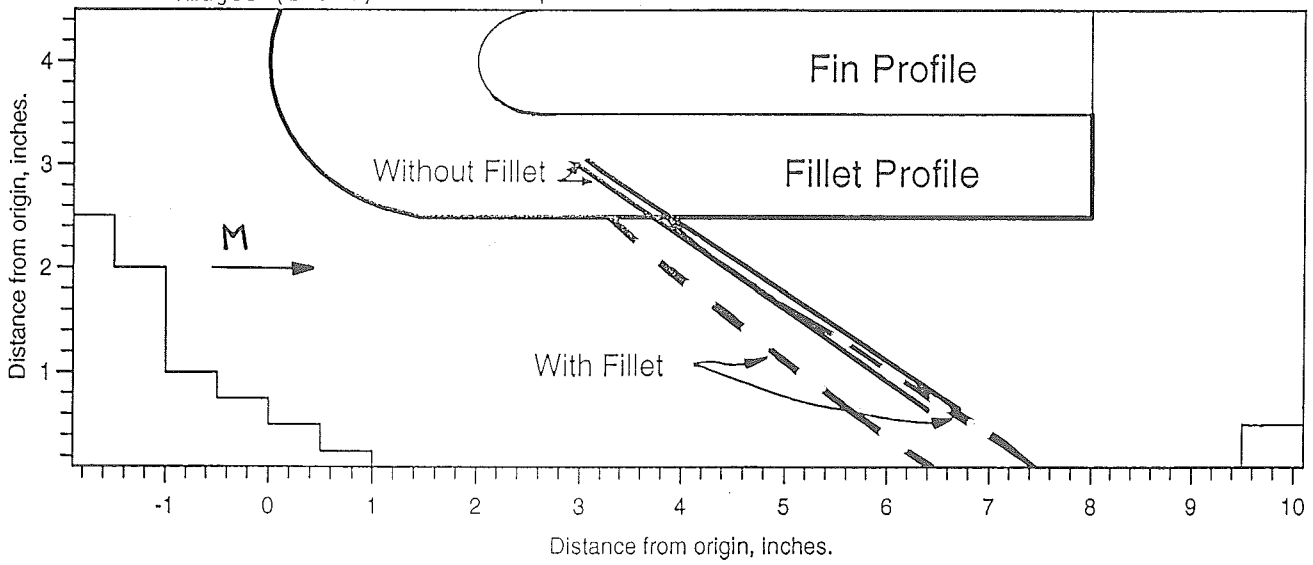

Fig. 20 Superimposing of the bow shocks for the swept models.